

## CHAPTER 72

### Toward A Simple Model of the Wave Breaking Transition Region in Surf Zones

David R. Basco<sup>1</sup> and Takao Yamashita<sup>2</sup>

#### Abstract

Breaking waves undergo a transition from oscillatory, irrotational motion, to highly rotational (turbulent) motion with some particle translation. On plane or monotonically decreasing beach profiles, this physically takes place in such a way that the mean water level remains essentially constant within the transition region. Further shoreward a rapid set-up takes place within the inner, bore-like region. The new surf zone model of Svendsen (1984) begins at this transition point and the new wave there contains a trapped volume of water within the surface roller moving with the wave speed. This paper describes a simple model over the transition zone designed to match the Svendsen (1984) model at the end of the transition region. It uses a simple, linear growth model for the surface roller area development and semi-empirical model for the variation of the wave shape factor. Breaking wave type can vary from spilling through plunging as given by a surf similarity parameter.

The model calculates the wave height decrease and width of the transition region for all breaker types on plane or monotonically depth decreasing beaches.

#### 1.0 Introduction

A general understanding of the mean flow fields in the transition region of breaking-broken water waves has yet to be achieved. The wave character undergoes a transformation from irrotational, orbital particle motion to rotational, highly turbulent motion with some particle translation. We shall herein define the transition region width from the break point to the point (transition point) where the mean water surface changes from essentially level to an increasing slope (wave set-up). This paper presents relatively simple relationships to calculate the wave height decrease and width of the transition region for plane beaches.

After the transition, the broken wave propagates as a moving bore containing a trapped volume of water in the surface roller moving with the wave speed (Svendsen, 1984). Plunging breakers have an identifiable plunge point where the overturning, falling jet impacts the oncoming trough. Thereafter, a relatively short and violent flow redistribution occurs to develop the bore-like wave character. Spilling breakers have essentially zero plunge distance to begin rotation, but then a relatively long and gradual flow redistribution

---

<sup>1</sup>Professor Civil Engineering and Director, Coastal Engineering  
Institute, Old Dominion Univ., Norfolk, VA 23508

<sup>2</sup>Instructor, Disaster Prevention Research Institute, Kyoto University  
Kyoto 611, Japan.

takes place over the water column. In general, the transition width for spilling breakers is greater than for plunging breakers. We shall tacitly assume that the end of the transition region for both plungers and spillers is also identifiable by the bore-like character of the broken wave within the inner-surf zone region.

Wave height change within and the width of the transition region are not insignificant quantities. Figure 1 shows the wave height,  $H$ ; celerity,  $c$ ; and mean water level,  $\bar{\eta}$  (set-down, set-up) variations before and through the surf zone (courtesy J. Buhr Hansen) for laboratory scale waves breaking on a plane beach. Zone I is the transition region where  $\bar{\eta}$  is (relatively) constant. In this example, roughly one-third of the wave height decrease takes place in a transition distance that is approximately one-quarter of the surf zone width. Galvin (1969) presented a method to estimate the plunge distance from laboratory data on plane beaches. Visser (1984) developed a mathematical model for the wave-induced longshore current which critically hinged on the physical fact that dissipation of wave energy begins at the plunge point and not over the entire surf zone. His laboratory experiments for plunging breakers resulted in plunge distances ranging from 22-43% of the total surf zone width. By definition, the transition width will be an even greater percentage.

We limit this discussion to waves breaking on plane or monotonically (depth) decreasing beaches. In deep water or for waves breaking on bars, the excessive depths after the break point will result in completely different internal physical processes. A fully developed, bore-like wave character may never be achieved, the mean water level may not stay constant and consequently, the transition width may have to be redefined.

## 2.0 Qualitative Description

A qualitative description of processes and mechanisms within the transition region has been presented by Basco (1985). Both classic spilling and plunging type breakers were found to have similar initial breaking motions, but at vastly different scales. Two primary vortex motions were identified. A plunger vortex is initially created by the overturning jet, which in turn causes a splash-up of trough fluid and subsequent formation of a surface vortex of similar scale. Figure 2 schematically depicts a strong plunging breaker. For plunging breakers, this plunger vortex translates laterally to push up a new surface wave with new wave kinematics that continues propagating into the inner surf zone. For spilling breakers, the small scale plunger vortex creates a small scale disturbance masked by the larger carrier wave. However, the resulting surface roller at the crest slides down and grows in size on the face of the main wave. The end result is also a new wave kinematic structure.

This sequence of events is schematically depicted in Figure 3 for a plunging breaker. Two new key features were introduced for the first time by Basco (1985). The overturning jet is deflected down and to the rear by the onrushing trough to create a rotating fluid mass system (steps 1-5). This plunger vortex translates horizontally much

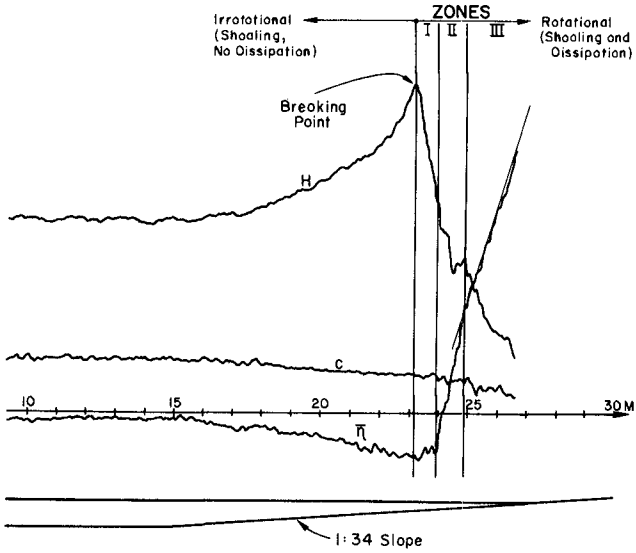


Fig. 1 Example of wave height, celerity and mean water level variations before and after breaking (Test No. 053074 courtesy J. Buhr Hansen, 1982)

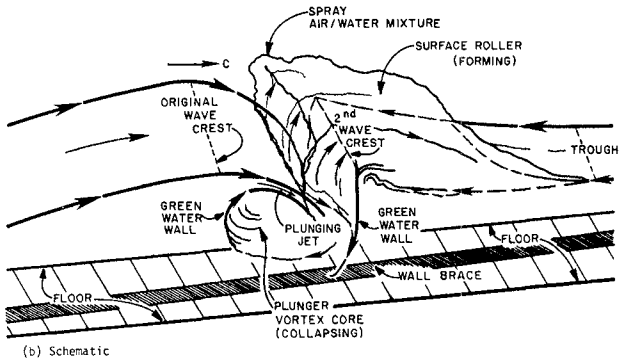


Fig. 2 Schematic of strong plunging breaker

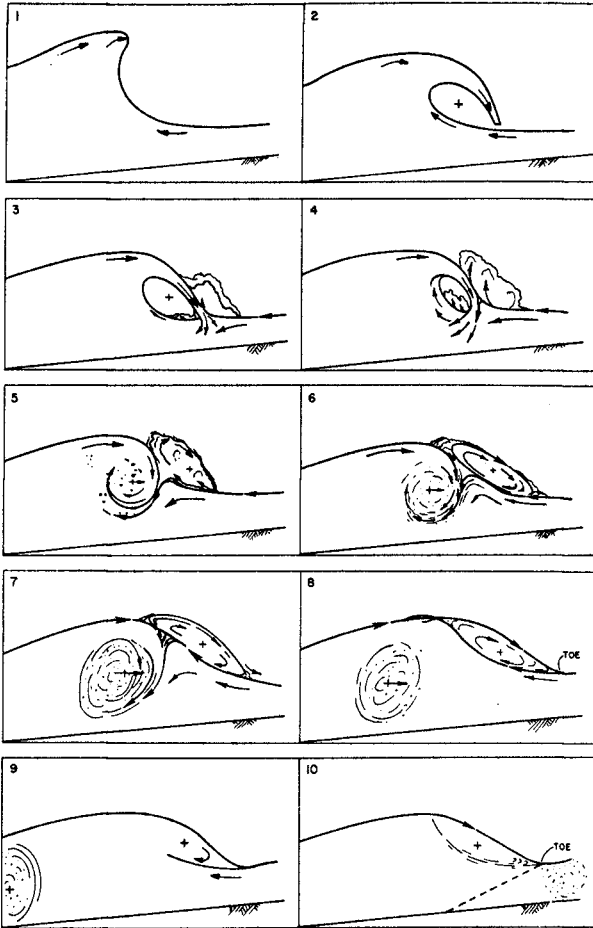


Fig. 3 Schematic sequence of breaking wave events (From Basco, 1985)

like a piston wave board to push up a rising water surface and simultaneously create a new, secondary surface disturbance (5-8). The plunger vortex comes to rest and is left behind which marks the end of the original propagating wave (8-10). The transition point occurs somewhere near step 8.

A new wave has been created (9-10) with kinematic structure that results from mean momentum redistribution and turbulence transport in both vertical and horizontal dimensions. Turbulence production, advection, diffusion and dissipation are locally in a nonequilibrium state. The turbulent redistribution of the mean, internal velocity field results in a trapped, concentration of mass within the surface roller that moves with the wave. Beneath the roller, fluid particles retain their orbital character but in a highly turbulent state.

The transition region can now be viewed as the zone where the original, irrotational, wave like motion comes to rest and simultaneously generates a new, secondary, bore-like wave with completely different wave kinematics as in the Svendsen (1984) model discussed below.

### 3.0 Recent Theory and Paradoxes

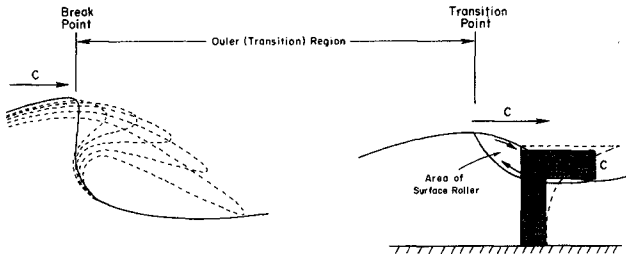
The surf zone model of Svendsen (1984) begins at the transition point. Here, the mean velocity profile relative to a fixed observer is as shown by the dashed line in Figure 4 and area, A. Svendsen found a correlation between A and wave height squared from laboratory data as shown in Figure 4b. The presence of the trapped surface roller was modeled by the simple velocity profile (Figure 4b) and significantly altered both the momentum flux (radiation stress) and energy flux over that determined by linear wave theory. In fact, the radiation stress,  $S_{xx}$  increased by 50-100% and the energy flux,  $E_f$  essentially doubled.

The resulting conservation equations when solved together permitted calculation of the wave height decrease and mean water surface increase across the inner region. An example comparison of theory (solid line) and laboratory experimental data is reproduced as Figure 5 (from Svendsen, 1984). Note that the theory begins at the transition point, not at the break point. And, that the theory without the surface roller effect (dashed line) gives incorrect results.

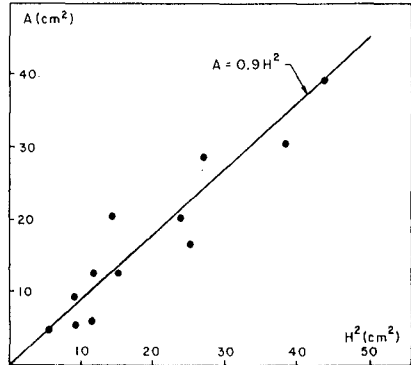
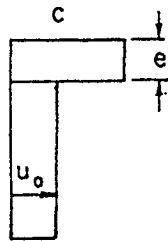
Consider the cross-shore momentum balance equation for depth-integrated and time-averaged wave motion

$$\frac{dS_{xx}}{dx} + \rho g h \frac{d\bar{\eta}}{dx} = 0 \quad (1)$$

where:  $h = \bar{\eta} + d$ , the mean water depth,  
 $d$  = the still water depth,  
 $\bar{\eta}$  = the mean water level change (set-up, set-down),  
 $\rho$  = the fluid mass density, and  
 $g$  = the gravitational acceleration.



(a) Velocity profile at end of transition (transition point)



(b) Correlation between surface roller area and wave height,  $H^2$  (from Svendsen, 1984)

Fig. 4 Schematic of wave breaking profiles through transition region

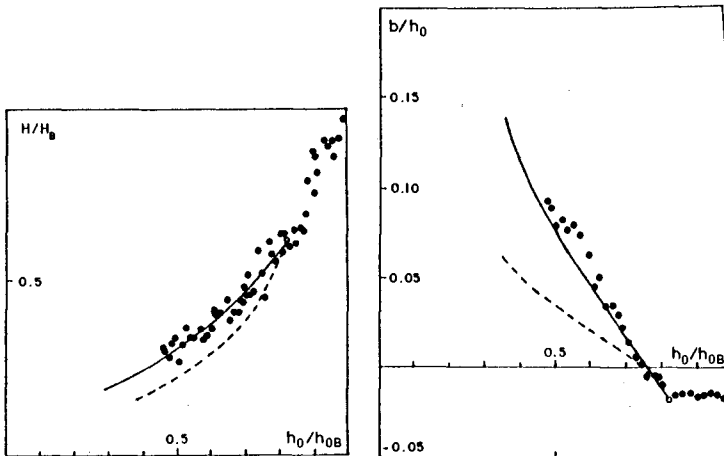


Fig. 5 Wave heights and set-up for a wave with deep water steepness (From Svendsen, 1984, Fig. 13, p. 322)

The data in Figures 1 and 5 reveal that  $\bar{\eta}$  is essentially constant across the transition region. This means from Eqn. (1) that  $S_{xx}$  is proportional to the wave height squared (e.g. Longuet-Higgins and Stewart, 1964). This presents a paradox. How can  $\bar{\eta}$  (i.e.  $S_{xx}$ ) remain constant when H decreases rapidly across the transition region? We shall return to this point below.

A second point of emphasis concerns the common misconception that breaking wave height decrease is solely due to energy dissipation through turbulence. Using time-averaged conservation laws of momentum and energy across the transition region considered as one control volume (analogous to the hydraulic jump), Svendsen (1984) demonstrated that about one-third of the energy change due to wave height decrease was actually lost as dissipation. The remaining two-thirds was energy redistribution between potential (pressure) and kinetic (velocity) forms. Thus to continue to view wave breaking as the same wave propagating with some energy dissipation is to miss the fundamental physical transition taking place internally between the velocity and pressure related terms in the momentum and energy balance equations.

**4.0 Elements of a Simple Quantified Model**

It is instructive to first quantify the momentum flux distribution due to velocity and pressure related components across a steady hydraulic jump.

**4.1 Stationary Hydraulic Jump**

The total momentum, m (per unit mass density and sectional area) at any section before, within, and after a hydraulic jump can be written

$$m = m_v + m_p \tag{2}$$

or

$$m = \frac{\alpha q^2}{d} + \frac{1}{2} g d^2 \tag{3}$$

where:  $q \equiv \int_0^d u dz$ , the volumetric flowrate,  
 $u$  = the horizontal velocity component,  
 $d$  = the local water depth,  
 $z$  = the vertical coordinate, and

$$\alpha \equiv \frac{d}{q^2} \int_0^d u^2 dz, \text{ the momentum correction coefficient.}$$

Total momentum is the sum of that due to velocity,  $m_v$  and that due to an assumed hydrostatic pressure distribution,  $m_p$ .

Using the definition of a Froude number, F along with known jump entrance conditions,  $u_1, d_1$ , it can be easily show that

$$\frac{m_{v1}}{m} = \frac{F_1^2}{F_1^2 + \frac{1}{2}} \tag{4}$$

from which it follows that

$$\frac{m_{p1}}{m} = 1 - \frac{m_{v1}}{m} \quad (5)$$

From the sequent-depth equation the subcritical downstream depth,  $d_2$ , can be determined and similar expressions for  $m_{v2}$  and  $m_{p2}$  established in terms of  $F_2$ . The key fact is that total momentum,  $m$  is constant across the hydraulic jump.

Svendsen and Madison (1983) present a new hydraulic jump theory in which the momentum correction coefficient,  $\alpha$  is given by the relationship

$$\alpha = \zeta \left[ 1 + \frac{1}{2F_1^2} (1 - \zeta^2) \right] \quad (6)$$

where

$$\zeta = \frac{d(x)}{d_1}$$

Using their method, one can calculate  $d(x)$  for a given  $F_1$  and consequently, using (6), (3), (4) and (5), in that order, we can also calculate the theoretical partition of  $m_v$  and  $m_p$  across the jump. Figure 6 presents the results for some representative inlet Froude numbers. For example, when  $F_1=3$  almost 95% of the total momentum at the inlet is due to velocity and only 5% from pressure. Whereas, at the exit, now only 25% is velocity related while nearly 75% is due to pressure. We also see that the jump roller which contains a flow reversal creates  $\alpha > 1$  through the jump and is responsible for the nonlinear distributions of  $m_v$  and  $m_p$  components.

#### 4.2 Broken Waves in Inner Surf Zone Region

Next, consider the time-averaged and depth-integrated excess momentum flux, i.e. the radiation stress for the inner region. For the simplified velocity profile through the trapped surface roller (Fig. 4b), Svendsen (1984) found that

$$\begin{aligned} S_{xx} &= S_v + S_p \\ &= \left[ \rho g H^2 \left( B_0 + \frac{A}{H^2} \frac{h}{L} \right) + \frac{1}{2} \rho g H^2 B_0 \right] \end{aligned} \quad (7)$$

where

$L$  = the wave length, and

$$B_0 = \frac{1}{T} \int_0^T \frac{\eta^2}{H^2} dt \quad (8)$$

with

$T$  = the wave period.

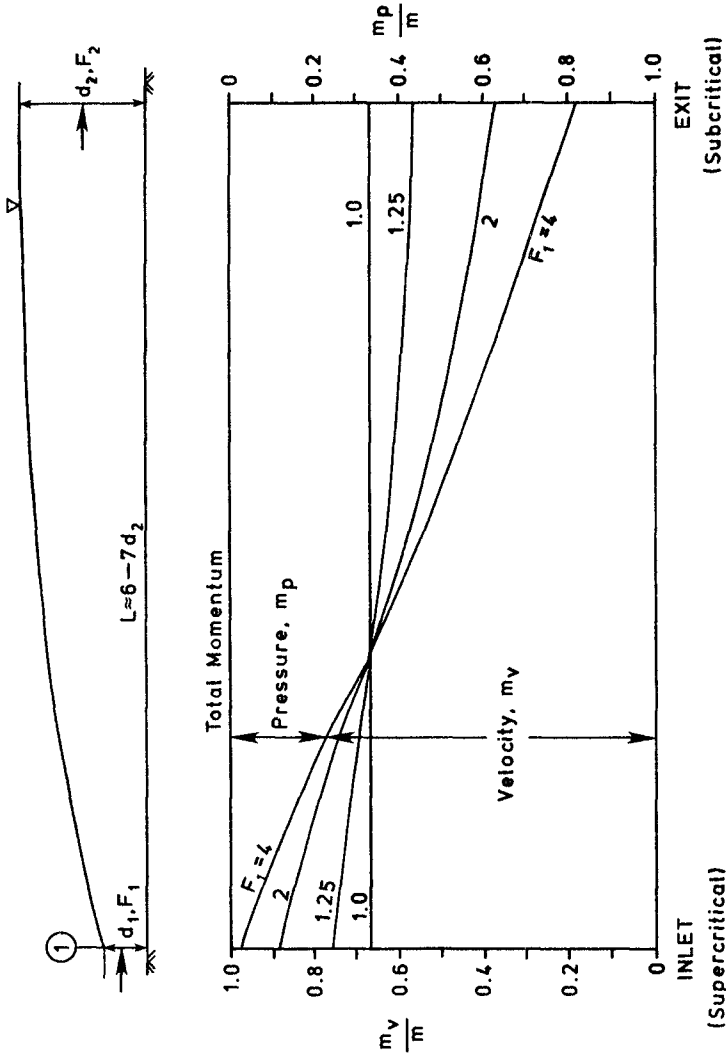


Fig. 6 Partition of velocity and pressure momentum components through a steady, hydraulic jump

$B_0$  is a wave surface shape factor discussed in further detail below. The first part of Equation (7) is that part of  $S_{xx}$  due to velocity,  $S_v$  and the latter is due to pressure,  $S_p$ . Recall that by definition,  $S_{xx}$  is the total flux of horizontal momentum across a vertical plane minus the stillwater hydrostatic pressure force. Hence the total force (per unit length) at any section is given by

$$M_{xx} = S_{xx} + \frac{1}{2} \rho g d^2 \quad (9)$$

This results in a total pressure related component,  $F_p$  for total momentum given by

$$\begin{aligned} F_p &= S_p + \frac{1}{2} \rho g d^2 \\ &= \frac{1}{2} \rho g H^2 B_0 + \frac{1}{2} \rho g d^2 \\ &= \frac{1}{2} \rho g (H^2 B_0 + d^2) \end{aligned} \quad (10)$$

As an example, consider the partition of a normalized radiation stress,  $P$  given by

$$\begin{aligned} P &= P_v \text{ (velocity)} + P_p \text{ (pressure)} \\ &= \frac{S_{xx}}{\rho g H^2} = \left( B_0 + \frac{A h}{H^2 L} \right) + \frac{1}{2} B_0 \end{aligned} \quad (11)$$

From typical values for plunging breakers, as given by Svendsen (1984) for  $A/H^2$ ,  $h/L$  and  $B_0$ , the ratio of  $P_v/P_p$  was about 3.5 at the transition point. This means that about 80% of the total excess momentum flux at the transition point is due to velocity. However, when total momentum is considered, the broken waves account for only 20% of the total present.

#### 4.3 Breaking/Broken Waves in Transition Region.

We now return to the first paradox, namely how the mean water level,  $\bar{\eta}$  and hence  $S_{xx}$  from Equation (1) can remain constant when  $H$  decreases rapidly across the transition region. From Equation (7) it becomes apparent that both the  $A/H^2$  ratio and  $B_0$  must vary considerably to keep  $S_{xx}$  at a constant level. In what follows we tacitly assume that  $h/L$  remains essentially constant within the transition region, for a give situation.

Surface Roller Area. For plunging breakers, the surface roller begins forming at the plunge point. For spillers, it grows in size right from the break point. No experimental information is available. We therefore assume a linear growth of the  $A/H^2$  ratio as depicted in Figure 7 from a zero level to a peak of 0.9 at the transition point. Consequently, we match the Svendsen (1984) model at the start of the inner surf zone region.

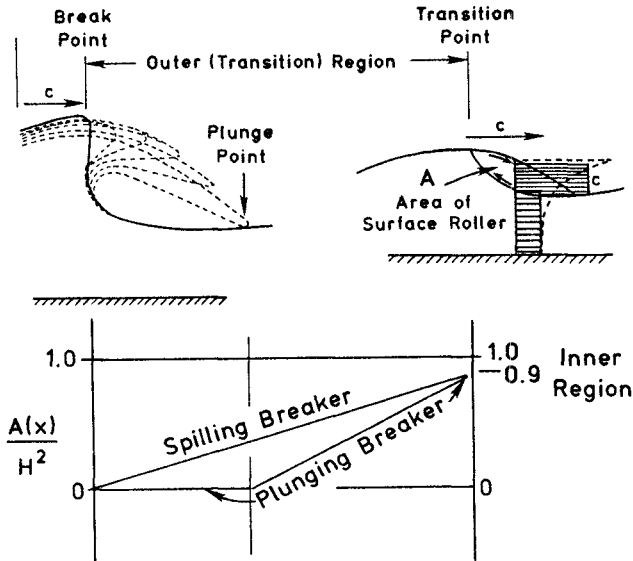


Fig. 7 Empirical  $A(x)/H^2$  distribution through transition region for spilling and plunging breakers

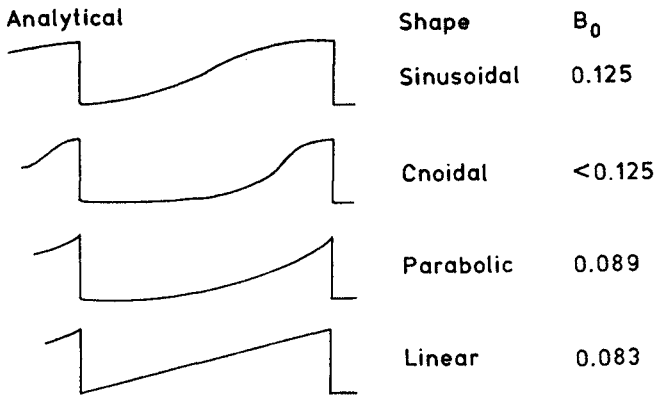


Fig. 8 Theoretical breaking wave shapes and resulting wave shape factor,  $B_0$  as defined by Eqn. (8)

Surface Shape Factor,  $B_0$ . Figure 8 depicts some possible breaking wave shapes (sinusoidal, cnoidal, parabolic, linear) that can all be treated analytically within Equation (8) to calculate theoretical values of  $B_0$  at the moment of wave breaking (vertical front face). The resulting  $B_0$  values are also shown in Figure 8 and are always less than 0.125.

Using the laboratory measurements of Hansen (1982), values of  $B_0$  for various positions across the surf zone were calculated by Svendsen (1984) as reproduced here in Figure 9. For this data, peaky wave profiles produced  $B_0$  values as low as 0.035 at the break point ( $h_0/h_{0b}=1.0$ ). Then,  $B_0$  values increased rapidly towards values around 0.06-0.09. Svendsen (1984) noted some variation of  $B_0$  with deep water steepness,  $H_0/L_0$ .

The surf similarity parameter (i.e., the Iribarren number) defined as

$$\xi = \frac{\text{Bottom Slope}}{(\text{Deep Water Steepness})^{1/2}} = \frac{\tan \beta}{(H_0/L_0)^{1/2}} \quad (12)$$

is useful to further quantify the possible  $B_0$  variations. Figure 10 presents combined theoretical and experimental results (Figure 9) in an heuristic fashion for  $B_0$  versus  $h_0/h_{0b}$  for spilling (small  $\xi$ ) through plunging (large  $\xi$ ) breakers.

In the wave shoaling region ( $h_0/h_{0b}>1$ ) the waves begin with near sinusoidal shape ( $B_0=0.125$ ) and are transformed in shape to become spilling (relatively high  $B_0$  values) or plunging (relatively low  $B_0$  values) breakers. Further theoretical results are needed using numerical wave shoaling simulations and experimentally determined data to further quantify this region.

After breaking ( $h_0/h_{0b}<1$ ) the experimentally measured results from Figure 9 have been replotted and smooth curves drawn in Figure 10. Much more experimental data is needed to confirm these trends. Ultimately, the smallest waves running up the beach return to a sinusoidal form. Figure 10 can be used to estimate  $B_0$  values for various positions ( $h_0/h_{0b}$ ) and wave types ( $\xi$ ) found in surf zones.

Transition Width,  $W$ . Figure 10 also shows a curve marking the width of the transition region. At best, this is only a very crude estimate based upon some limited data presented in Svendsen (1984). Spilling transitions are shown to be wider than plunging transition regions. Much further experimental and theoretical research is needed to quantify this estimate. For example, ongoing work is attempting to quantify the partition between momentum flux due to velocity and that due to pressure (wave induced plus static) in a reference frame moving with celerity,  $c$  across the transition region. When coupled with a proper energy dissipation model (recall second paradox above), it should be theoretically possible to predict the transition width. The procedure being followed is essentially that used by Madsen and Svendsen (1983) to calculate the length of the stationary hydraulic

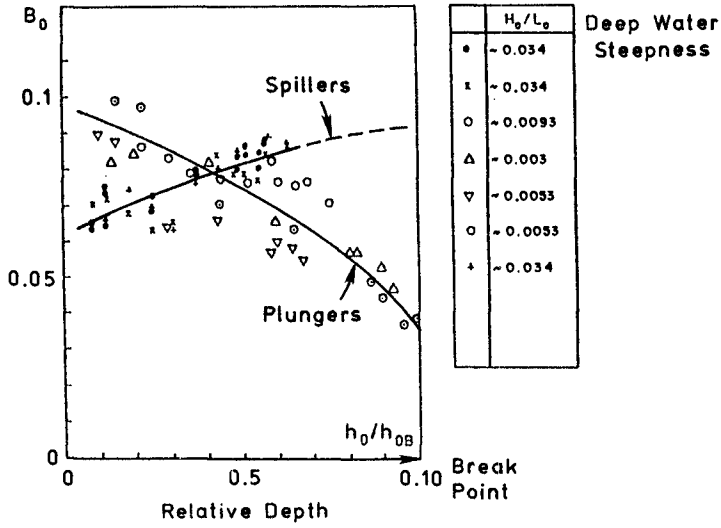


Fig. 9 Measured values of  $B_0$  as defined by Eqn. (8) (From Svendsen, 1984, Fig. 9, p. 316)

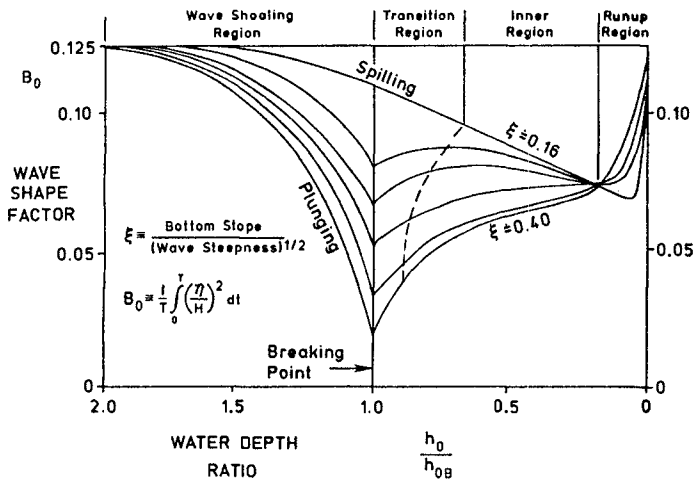


Fig. 10 Variation of wave shape factor,  $B_0$  before and after breaking of spilling through plunging type breakers

jump. Results of numerical model simulations of breaking wave overturning and jet falling up to the plunge point will be employed to calculate the plunge distance.

#### 4.4 An Example Computation

Equation (7) can be rewritten

$$S_{xx} = \rho g H^2 \left( \frac{3}{2} B_0 + \frac{A}{H^2} \frac{h}{L} \right) \quad (13)$$

Given the breaking wave height,  $H_b$ , the fluid mass density (fresh or sea water) and the  $(h/L)_b$  ratio at breaking, it is now possible to calculate the wave height decrease and width of the transition region. Keeping in mind, of course, these result are only for plane beaches. The key fact is that  $S_{xx}$  remains constant across the transition. Figure 7 and 10 are utilized to estimate the  $A(x)/H^2$  and  $B_0(x)$  variables required.

Plunging Breaker. Assume the deep water steepness ( $H_0/L_0$ ) and beach slope produce a similarity parameter,  $\xi$  equal to 0.35. This is a fairly strong plunging breaker. The computation proceeds as follows ( $H_b=2.5\text{m}$ , sea water,  $(h/L)_b=0.057$ ):

$$\begin{aligned} (B_0)_b &= 0.035 \\ A(x) &= 0 \\ (S_{xx})_b &= 0.32 \times 10^4 \text{ N} \\ A/H^2 &= 0.9 \\ (B_0)_T &= 0.045 \\ (S_{xx})_T &= 0.32 \times 10^4 \\ &= 10^4 H_T^2 \left[ \frac{3}{2}(0.045) + 0.9(0.057) \right] \\ H_T &= 1.6 \text{ m} \\ \therefore H_T/H_b &= 0.65 \end{aligned}$$

For all intermediate locations between  $H_b$  and  $H_T$ , use  $A$  equal to zero up to plunge point and Figure 7 beyond linear by interpolation. The resultant  $H(x)$  is nonlinear (Eqn. 13).

Spilling Breaker. Now assume the incoming wave gives  $\xi$  equal to about 0.2 on the same beach. Using the same values as before ( $H_b=2.5\text{m}$ , sea water,  $(h/L)_b=0.057$  gives:

$$\begin{aligned} (B_0)_b &= 0.10 \\ A(x) &= 0 \\ (S_{xx})_b &= 0.94 \times 10^4 \text{ N} \\ A/H^2 &= 0.9 \end{aligned}$$

$$\begin{aligned}(B_0)_T &= 0.09 \\ H_T &= 2.2 \text{ m} \\ \therefore H_T/H_b &= 0.88\end{aligned}$$

Now all intermediate points use linear interpolation for  $A(x)$ . The resulting  $H(x)$  curve is also nonlinear.

These results can now be used as input to the surf zone model of Svendsen (1984) to calculate the  $H(x)$  and  $h(x)$  distribution over the remainder of the surf zone.

### 5.0 Summary Conclusions

A simple, quasi-empirical model for the wave breaking transition region of plane and monotonically decreasing beach profiles has been developed. The nonlinear wave height decrease and transition width for various breaker types can be estimated. The key element in the model is the fact that the mean water level is constant. Consequently, the wave ray, radiation stress component is also constant. An empirical, linear formulation is postulated for the surface roller area development. And, a semi-empirical formulation is developed for the wave shape factor. These two variables are taken so that the resulting model matches that developed by Svendsen (1984) at the end of the transition region, i.e. the start of the inner, bore-like wave region. The weakest part of the model is the limited empirical data available to estimate the transition width.

The research effort is ongoing and now focusing on theoretical means to determine the transition width.

The model is limited to plane or monotonically decreasing beach profiles. But it is seen as a necessary first step to develop similar methods for bar/trough beaches.

### References

- Basco, D.R. (1980) A Qualitative Description of Wave Breaking, Journal of Waterway, Port, Coastal and Ocean Engineering, Vol. III, No. 2, March, pp. 171-188.
- Galvin, C.J. Jr. (1969) Breaker Travel and Choice of Design Wave Height, Journal WW2, Vol. 95, No. 2, May, pp. 175-200.
- Hansen, J.B. (1982) personal communication.
- Longuet-Higgins, M.S. and R.W. Stewart. (1964) Radiation Stress in Water Waves: A Physical Discussion With Applications, Deep-Sea Research, Vol. II, No. 4, Oxford, England, August, pp. 529-562.

- Madsen, P.A. and I.A. Svendsen (1983) Turbulent Bores and Hydraulic Jumps, Journal Fluid Mechanics, Vol. 129, pp. 1-25.
- Svendsen, I.A. (1984) Wave Heights and Set-up in a Surf Zone Coastal Engineering, Vol. 8, pp. 303-329.
- Visser, P.J. (1984) Uniform Longshore Current Measurements and Calculations, Proceedings, 19th ICCE, (Houston), Vol. III, pp. 2192-2207.